

Variation of Stress Concentration Around Rectangular Holes. Influence of Joints Types Between the Sides of a Rectangular Holes.

Victor L. Pop^{*1}, Maria L. Pop², Petru M. Cosobea³

^{1,2,3} *Technical University of Cluj-Napoca, Faculty of Civil Engineering. 15 C Daicoviciu Str., 400020, Cluj-Napoca, Romania*

(Received 10 July 2013; Accepted 30 September 2013)

Abstract

The content of the article refers to the analysis of the stress in the elastic tape laid down with holes of rectangular shape subjected to stretching. Geometry and loads are fixed elements and attached holes geometric parameters (shapes, sizes), parameters that characterize the cases studied. Results of the analysis, obtained using finite element method (FEM), is focused on mapping and stresses distributions, tables and graphs of the variation of the stress concentration factor, depending on the geometric parameters set. The analysis concerns rectangular tape with rectangular holes subjected to axial force. In the following analysis of the elastic tape, there are provided rectangular holes with circular or straight joints. In these cases, the benchmark of comparison using results from rectangular holes in the elastic tape without joints. It also makes a comparative analysis of circular joints and connections with infinite radius of curvature (chamfered joints). All results are accompanied by interesting and useful observations and conclusions for the effective design of such elements.

Rezumat

Conținutul principal al articolului se referă la analiza stării de tensiune în banda elastică, prevăzută cu goluri rectangulare, solicitată la întindere, respectiv la încovoiere. Sunt fixate geometria și încărcările elementelor, precum și parametrii geometrici variabili atașați golurilor (forme, dimensiuni), parametri care caracterizează cazurile studiate. Rezultatele analizei, obținute prin metoda elementului finit (MEF), se concretizează în hărți și distribuții de tensiuni, tabele și grafice de variație ale factorului de concentrare a tensiunilor, funcție de parametrii geometrici stabiliți. Analiza se referă la banda elastică cu goluri rectangulare, solicitată la forță axială. Următoarea analiza studiaza golurile rectangulare din banda elastică care sunt prevăzute cu racorduri circulare, respectiv racorduri drepte. În aceste cazuri, ca reper de comparație se folosesc rezultatele de la banda elastică cu goluri rectangulare fără racordări. Se face, de asemenea, o analiză comparativă între racordurile circulare și racordurile cu raza de curbură infinită (racordurile drepte). Toate rezultatele sunt acompaniate de observații și concluzii interesante și utile pentru proiectarea efectivă a unor astfel de elemente.

Keywords: stress concentration, finite element method, elastic tape, circular joints, straight joints

* Corresponding author: Tel./ Fax.: +40 264 522598
E-mail address: victorpop@mecon.utcluj.ro

1. Introduction

Stress distribution inside a homogeneous and isotropic frame is continuous and uniform. In a flat plate (rigid diaphragm) driven in its plan by evenly distributed tension forces from her outline, it occurs as an evenly distributed state of stresses. At bars with constant or variable section properties, studies according with The Theory of Elasticity and experiments had confirmed Bernoulli's plane sections hypothesis which drives to constant strains in case of axial loading, respectively linear variation in case of bent bars. The stress distribution (bending moments, torsion, shear) in a plate loaded perpendicular to its plan by evenly distributed forces is given also by continuous function. For structural elements stress concentrations appear most frequently in:

- along holes;
- at local cross-section variations (as in sudden cross section change, or joints along bars or plates);
- in elements where in some areas appear tangent or curvature discontinuities;
- discontinuities in the material property itself: non-metallic inclusions, fractures due to the fabrication process (welds or cold processing).

Non-uniform distribution of stress in the vicinity of a discontinuity occurs a local tension. By noting with σ_{max} the maximum stress of the discontinuity, is defined as the stress concentration factor, α_k , the ratio:

$$\alpha_k = \frac{\sigma_{max}}{\sigma_n} \quad (1)$$

where σ_n is the normal stress in a point that would occur in the absence of discontinuity. Stress σ_{max} can be determined analytically or experimentally. In the first case, α_k is called analytical or calculated concentration factor, in the second case, the factor obtained is denoted by α_{kE} and call it experimental or actual concentration factor.

2. Analysis of elastic tape with rectangular holes

2.1. The elastic tape with rectangular holes provided with circular joints.

Analysis of circular joints on the state of stress in the *elastic tape* will perform on a plate thickness $t = 1$, the form in the XY plane is shown in Figure 1. To simulate the loading of the tape at $x = \pm\infty$ we chose a length of $L = 5h$ so that local stress should be limited central area $|x| \ll L/2$ (according to the principle of S. Venant). We focused out attention on the study of stress concentration aspects for a square located in central position with $d \times d$ size and having different circular radius joints between its sides. Geometric modeling is characterized by the following parameters:

- the ratio between the size of the hole and the width of the tape (d/h)
- the ratio between the size of circular radius joints and the size of the hole ($f(r)/d$)
- the hole placement is situated on the tape central position.

The unit thickness tape was loaded at $x = \mp L/2$ (Figure 1) with constant stress of σ_x ($\sigma_x = 1000kN/m$ simulating axial load N at $x = \pm\infty$)

$\sigma_x = 1000kN/m$

$\sigma_x = 1000kN/m$

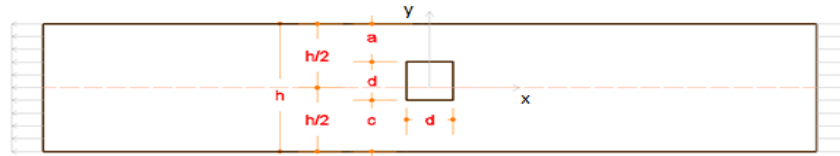


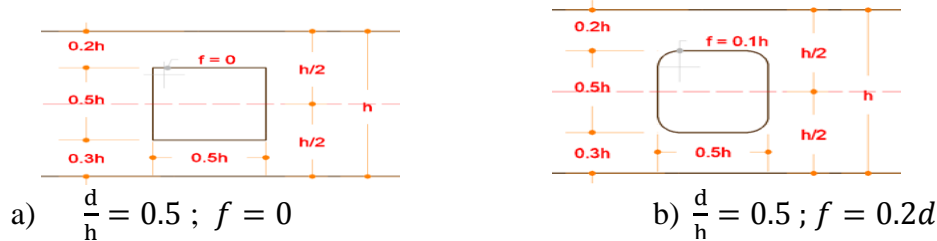
Figure 1. Geometric characteristic of elastic tape.

Four dimensions were chosen for the circular radius joints ($f = 0.1 d, 0.2 d, 0.3d, 0$), for the five cases previously analyzed with different rectangular hole dimensions ($d / h = 0.1, d / h = 0.2, d / h = 0.3, d / h = 0.5, d / h = .75$). Thus the 20 cases of analysis results, are presented in Table 3.4.

		<i>f</i> (circular joints)			
		0,1 <i>d</i>	0,2 <i>d</i>	0,3 <i>d</i>	0
$\frac{d}{h}$	0.1	0,01	0,02	0,03	0
	0.2	0,02	0,04	0,06	0
	0.3	0,03	0,06	0,09	0
	0.5	0,05	0,1	0,15	0
	0.75	0,075	0,15	0,225	0

Table 1. Different square holes dimension and circular joints.

Exemplifying the variation of circular radius joints of the tapes with ratio $d/h = 0.5$ are shown in Figure 2.

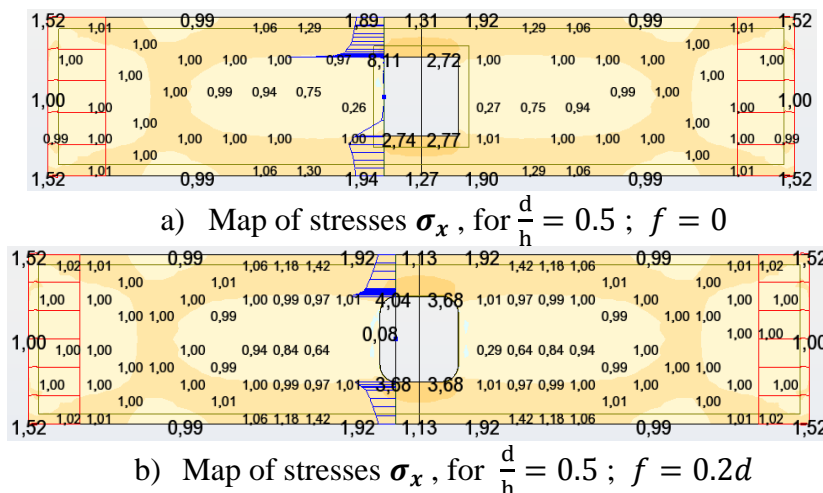


a) $\frac{d}{h} = 0.5 ; f = 0$

b) $\frac{d}{h} = 0.5 ; f = 0.2d$

Figure 2. Variation of circular radius joints dimensions.

Figure 2 is exemplified how the stress distribution σ_x in the elastic tape with rectangular holes having four different variations of circular radius joints, with the ratio $d/h = 0.5$ loaded with axial uniform distributed force.



a) Map of stresses σ_x , for $\frac{d}{h} = 0.5 ; f = 0$

b) Map of stresses σ_x , for $\frac{d}{h} = 0.5 ; f = 0.2d$

Figure 3. Stress distribution σ_x

Values of stresses in the elastic tape subjected to stretching for different circular radius joints between the sides of the hole																		
		$\alpha=a/h$	$\delta=d/h$	$\Upsilon=c/h$	$\zeta=z/h$	$\eta=I/h^3$	$\sigma_{max}(Mpa)$				$\sigma_{nom}(Mpa)$				α_k			
							σ_D	σ_c	σ_B	σ_A	σ_D	σ_c	σ_B	σ_A	A	B	C	D
0,75	f = 0	0,125	0,75	0,125	0,5	0,185	3,67	10,5	10,5	3,67	1,000	1,000	1,000	1,000	3,67	10,50	10,50	3,67
	f = 0,1	0,125	0,75	0,125	0,5	0,185	3,21	5,6	5,6	3,21	1,000	1,000	1,000	1,000	3,21	5,60	5,60	3,21
	f = 0,2	0,125	0,75	0,125	0,5	0,185	3,15	4,54	4,54	3,15	1,000	1,000	1,000	1,000	3,15	4,54	4,54	3,15
	f = 0,3	0,125	0,75	0,125	0,5	0,185	2,87	4,38	4,38	2,87	1,000	1,000	1,000	1,000	2,87	4,38	4,38	2,87
0,5	f = 0	0,25	0,5	0,25	0,5	0,344	1,63	6,35	6,35	1,63	1,000	1,000	1,000	1,000	1,63	6,35	6,35	1,63
	f = 0,1	0,25	0,5	0,25	0,5	0,344	1,49	3,83	3,83	1,49	1,000	1,000	1,000	1,000	1,49	3,83	3,83	1,49
	f = 0,2	0,25	0,5	0,25	0,5	0,344	1,34	3,42	3,42	1,34	1,000	1,000	1,000	1,000	1,34	3,42	3,42	1,34
	f = 0,3	0,25	0,5	0,25	0,5	0,344	1,19	3,24	3,24	1,19	1,000	1,000	1,000	1,000	1,19	3,24	3,24	1,19
0,3	f = 0	0,35	0,3	0,35	0,5	0,482	1,1	5,23	5,23	1,1	1,000	1,000	1,000	1,000	1,10	5,23	5,23	1,10
	f = 0,1	0,35	0,3	0,35	0,5	0,482	1,07	3,58	3,58	1,07	1,000	1,000	1,000	1,000	1,07	3,58	3,58	1,07
	f = 0,2	0,35	0,3	0,35	0,5	0,482	1,02	3,1	3,1	1,02	1,000	1,000	1,000	1,000	1,02	3,10	3,10	1,02
	f = 0,3	0,35	0,3	0,35	0,5	0,482	0,98	2,62	2,62	0,98	1,000	1,000	1,000	1,000	0,98	2,62	2,62	0,98
0,2	f = 0	0,4	0,2	0,4	0,5	0,555	1,01	5,01	5,01	1,01	1,000	1,000	1,000	1,000	1,01	5,01	5,01	1,01
	f = 0,1	0,4	0,2	0,4	0,5	0,555	1	3,48	3,48	1	1,000	1,000	1,000	1,000	1,00	3,48	3,48	1,00
	f = 0,2	0,4	0,2	0,4	0,5	0,555	0,99	2,97	2,97	0,99	1,000	1,000	1,000	1,000	0,99	2,97	2,97	0,99
	f = 0,3	0,4	0,2	0,4	0,5	0,555	0,98	2,54	2,54	0,98	1,000	1,000	1,000	1,000	0,98	2,54	2,54	0,98
0,1	f = 0	0,45	0,1	0,045	0,5	0,631	1	3,25	3,25	1	1,000	1,000	1,000	1,000	1,00	3,25	3,25	1,00
	f = 0,1	0,45	0,1	0,045	0,5	0,631	1	2,88	2,88	1	1,000	1,000	1,000	1,000	1,00	2,88	2,88	1,00
	f = 0,2	0,45	0,1	0,045	0,5	0,631	1	2,65	2,65	1	1,000	1,000	1,000	1,000	1,00	2,65	2,65	1,00
	f = 0,3	0,45	0,1	0,045	0,5	0,631	0,99	2,24	2,24	0,99	1,000	1,000	1,000	1,000	0,99	2,24	2,24	0,99

Table 2. Values of stresses in the elastic tape subjected to stretching for different circular radius joints between the sides of the hole

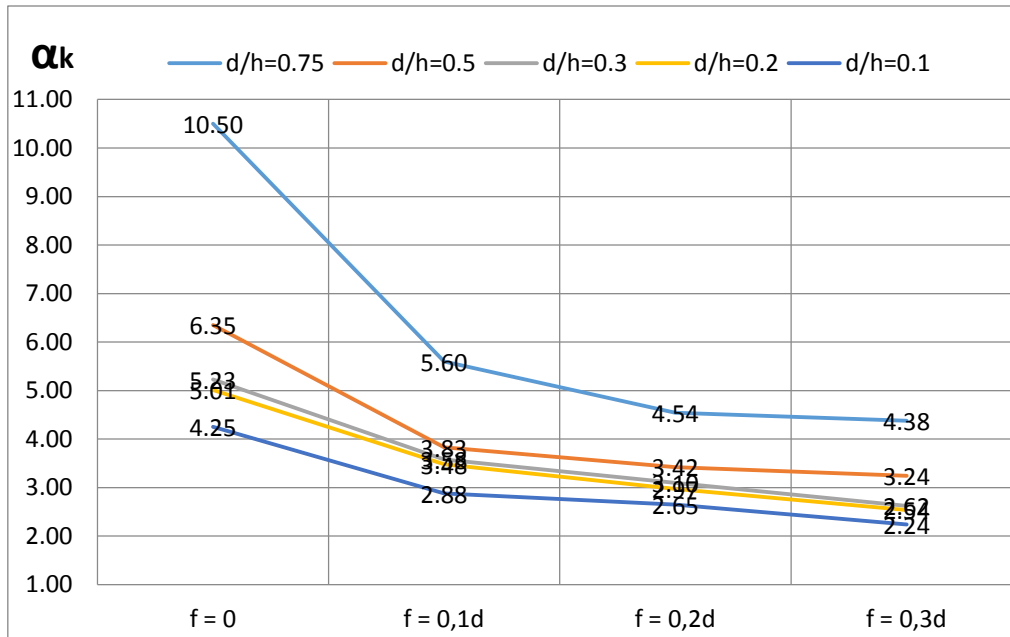


Figure 4. Variation of stress concentration factor α_k in the case of arbitrarily sized hole with different circular radius joints.

2.2. The elastic tape with rectangular holes provided with chamfered joints.

Analysis of chamfered joints on the state of stress in the elastic tape will perform on a plate thickness $t = 1$, the form in the XY plane is shown in Figure 3. To simulate the loading of the tape at $x = \pm\infty$ we chose a length of $L = 5h$ so that local stress should be limited central area $|x| \ll L/2$ (according to the principle of S. Venant). We focused out attention on the study of stress concentration aspects for a square located in central position with $d \times d$ size and having different circular radius joints between its sides.

Geometric modeling is characterized by the following parameters:

- the ratio between the size of the hole and the width of the tape (d/h)
- the ratio between the size of the chamfer joints and the size of the hole ($f(r)/d$)
- the hole placement is situated on the tape central position.

The unit thickness tape was loaded at $x = \mp L/2$ (Figure 5) with constant stress of ($\sigma_x = 1000kN/m$ simulating axial load N at $x = \mp\infty$).

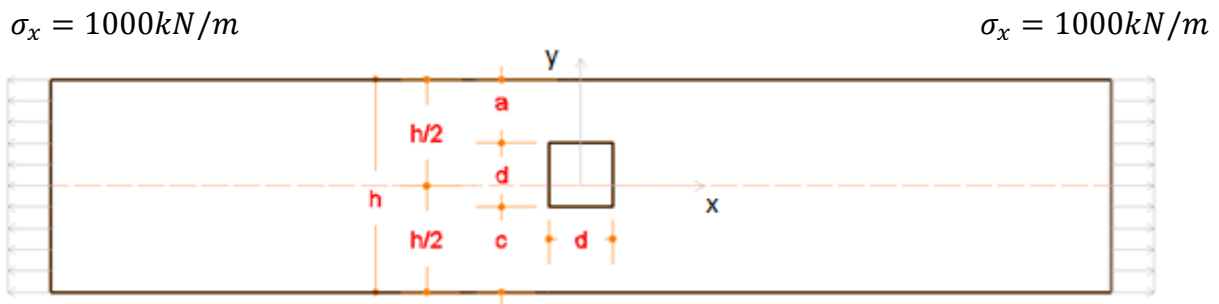


Figure 5. Geometric characteristic of elastic tape.

Four dimensions were chosen for the chamfered joints ($f = 0.1 d, 0.2 d, 0.3d, 0$), for the five cases previously analyzed with different rectangular hole dimensions ($d / h = 0.1, d / h = 0.2, d / h = 0.3, d / h = 0.5, d / h = .75$). Thus the 20 cases of analysis results, are presented in Table 3.

Table 3. Different square holes dimension and circular joints.

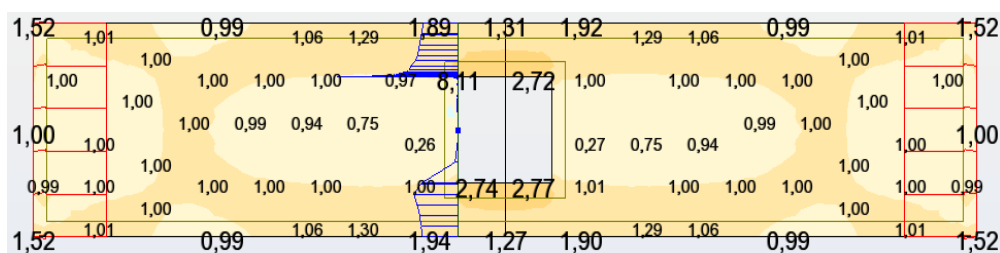
		<i>f</i> (chamfered joitns)			
		0,1 <i>d</i>	0,2 <i>d</i>	0,3 <i>d</i>	0
$\frac{d}{h}$	0.1	0,01	0,02	0,03	0
	0.2	0,02	0,04	0,06	0
	0.3	0,03	0,06	0,09	0
	0.5	0,05	0,1	0,15	0
	0.75	0,075	0,15	0,225	0

Exemplifying the variation of chamfered joints of the tapes with ratio $d/h = 0.5$ are shown in Figure 6.

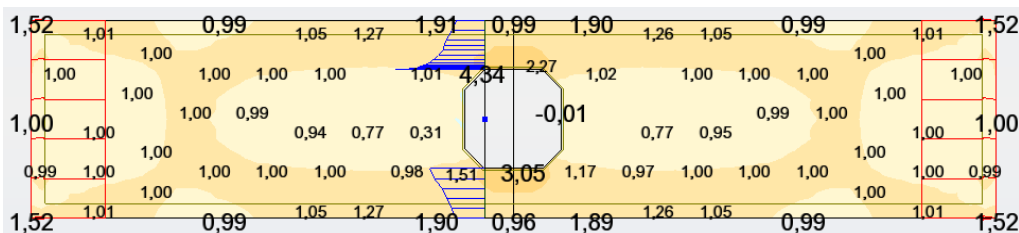


Figure 6. Variation of chamfered joints dimensions.

In figure 7 is exemplified how the stress distribution σ_x in the elastic tape with rectangular holes having four different variations of chamfer joints, with the ratio $d / h = 0.5$ loaded with axial uniform distributed force.



a) Map of stresses σ_x , for $\frac{d}{h} = 0.5 ; f = 0$



b) Map of stresses σ_x , for $\frac{d}{h} = 0.5 ; f = 0.2d$

Figure 7. Stress distribution σ_x .

Table 4. Values of stresses in the elastic tape subjected to stretching for different chamfered joints between the sides of the hole.

Values of stresses in the elastic tape subjected to stretching for different chamfered joints between the sides of the hole																		
	$\alpha=a/h$	$\delta=d/h$	$\gamma=c/h$	$\zeta=z/h$	$\eta=l/h^3$	$\sigma_{\max}(\text{Mpa})$				$\sigma_{\text{nom}}(\text{Mpa})$				α_k				
						σ_D	σ_c	σ_B	σ_A	σ_D	σ_c	σ_B	σ_A	A	B	C	D	
0,75	f = 0	0,125	0,75	0,125	0,5	0,185	3,67	10,5	10,5	3,67	1,000	1,000	1,000	1,000	3,67	10,50	10,50	3,67
	f = 0,1d	0,125	0,75	0,125	0,5	0,185	3,17	6,3	6,3	3,17	1,000	1,000	1,000	1,000	3,17	6,30	6,30	3,17
	f = 0,2d	0,125	0,75	0,125	0,5	0,185	2,85	5,78	5,78	2,85	1,000	1,000	1,000	1,000	2,85	5,78	5,78	2,85
	f = 0,3d	0,125	0,75	0,125	0,5	0,185	2,46	5,53	5,53	2,46	1,000	1,000	1,000	1,000	2,46	5,53	5,53	2,46
0,5	f = 0	0,25	0,5	0,25	0,5	0,344	1,63	6,35	6,35	1,61	1,000	1,000	1,000	1,000	1,63	6,35	6,35	1,61
	f = 0,1	0,25	0,5	0,25	0,5	0,344	1,47	5,35	5,35	1,47	1,000	1,000	1,000	1,000	1,47	5,35	5,35	1,47
	f = 0,2	0,25	0,5	0,25	0,5	0,344	1,27	4,42	4,42	1,27	1,000	1,000	1,000	1,000	1,27	4,42	4,42	1,27
	f = 0,3	0,25	0,5	0,25	0,5	0,344	1,01	4,16	4,16	1,01	1,000	1,000	1,000	1,000	1,01	4,16	4,16	1,01
0,3	f = 0	0,35	0,3	0,35	0,5	0,482	1,1	5,23	5,23	1,1	1,000	1,000	1,000	1,000	1,10	5,23	5,23	1,10
	f = 0,1	0,35	0,3	0,35	0,5	0,482	1,05	4,69	4,69	1,05	1,000	1,000	1,000	1,000	1,05	4,69	4,69	1,05
	f = 0,2	0,35	0,3	0,35	0,5	0,482	1	4,24	4,24	1	1,000	1,000	1,000	1,000	1,00	4,24	4,24	1,00
	f = 0,3	0,35	0,3	0,35	0,5	0,482	0,96	3,81	3,81	0,96	1,000	1,000	1,000	1,000	0,96	3,81	3,81	0,96
0,2	f = 0	0,4	0,2	0,4	0,5	0,555	1,01	5,01	5,01	1,01	1,000	1,000	1,000	1,000	1,01	5,01	5,01	1,01
	f = 0,1	0,4	0,2	0,4	0,5	0,555	1	4,51	4,51	1	1,000	1,000	1,000	1,000	1,00	4,51	4,51	1,00
	f = 0,2	0,4	0,2	0,4	0,5	0,555	0,99	3,74	3,74	0,99	1,000	1,000	1,000	1,000	0,99	3,74	3,74	0,99
	f = 0,3	0,4	0,2	0,4	0,5	0,555	0,97	3,68	3,68	0,97	1,000	1,000	1,000	1,000	0,97	3,68	3,68	0,97
0,1	f = 0	0,45	0,1	0,045	0,5	0,631	1	4,25	4,25	1	1,000	1,000	1,000	1,000	1,00	4,25	4,25	1,00
	f = 0,1	0,45	0,1	0,045	0,5	0,631	1	3,63	3,63	1	1,000	1,000	1,000	1,000	1,00	3,63	3,63	1,00
	f = 0,2	0,45	0,1	0,045	0,5	0,631	0,99	3,59	3,59	0,99	1,000	1,000	1,000	1,000	0,99	3,59	3,59	0,99
	f = 0,3	0,45	0,1	0,045	0,5	0,631	0,99	3,57	3,57	0,99	1,000	1,000	1,000	1,000	0,99	3,57	3,57	0,99

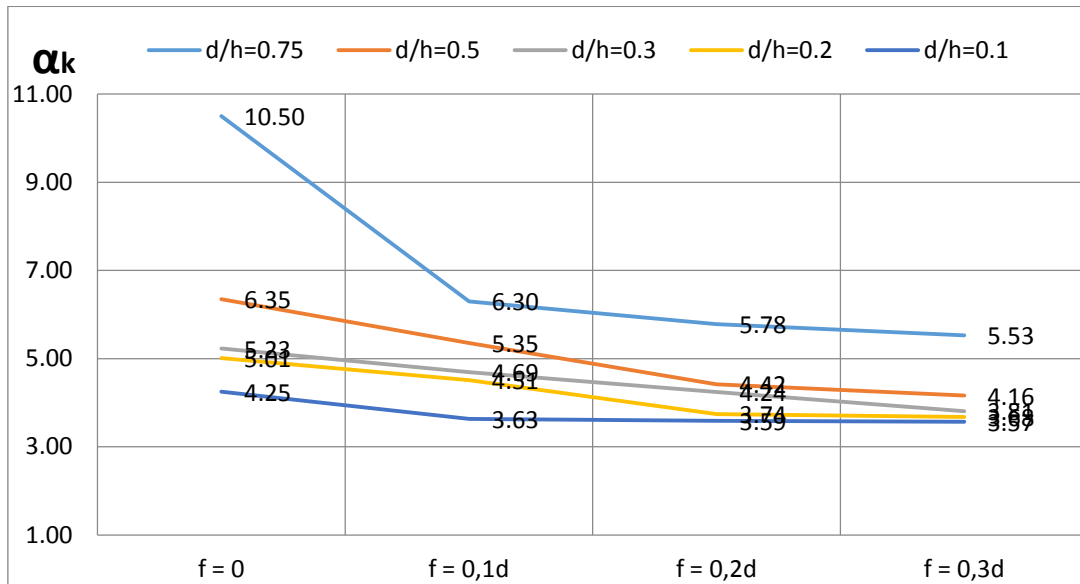


Figure 8. Variation of stress concentration factor α_k in the case of arbitrarily sized hole with different chamfered joints.

In Figure 8 we can see the influence of rectangular hole dimensions and chamfered joints on the values of α_k . From the graph we deduce a considerable influence of chamfered joints size on coefficient α_k in all studied cases. It can also be observed that the relation between size of rectangular holes and stress values is proportional.

2.3. Comparison between circular joints and chamfered joints in case of rectangular holes.

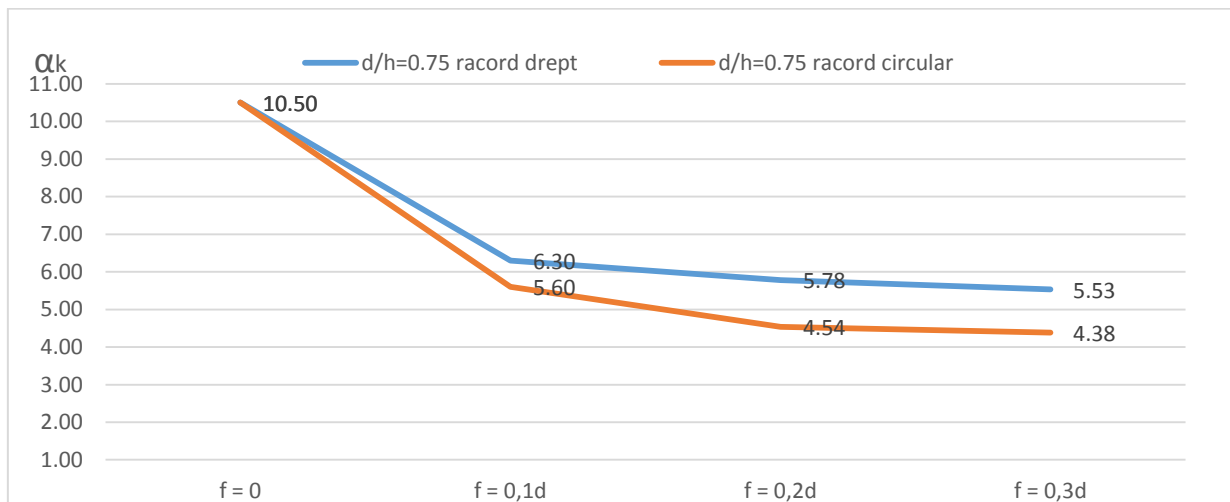


Figure 9. α_k values for d/h = 0.75

In Figure 9 are shown the values of α_k for central hole size $d / h = 0.75$ for both circular joints and chamfered joints. Note that the maximum values for α_k is when $f = 0$. α_k values are higher in the case of chamfered joints than in the case of circular joints with values of α_k lower with 12,5% in the case of chamfer joints for $f = 0.1d$, 27,3% for $f = 0.2d$ and 26,26% for $f = 0.3d$. Note in both cases a decrease α_k coefficient around rectangular holes with increasing size of the joint dimension. In this case we observe a sharp decrease in the coefficient α_k with the use of joints (either chamfered or circular joints). This reveals that the use of a certain type of joints leads to reduced stress around rectangular holes.

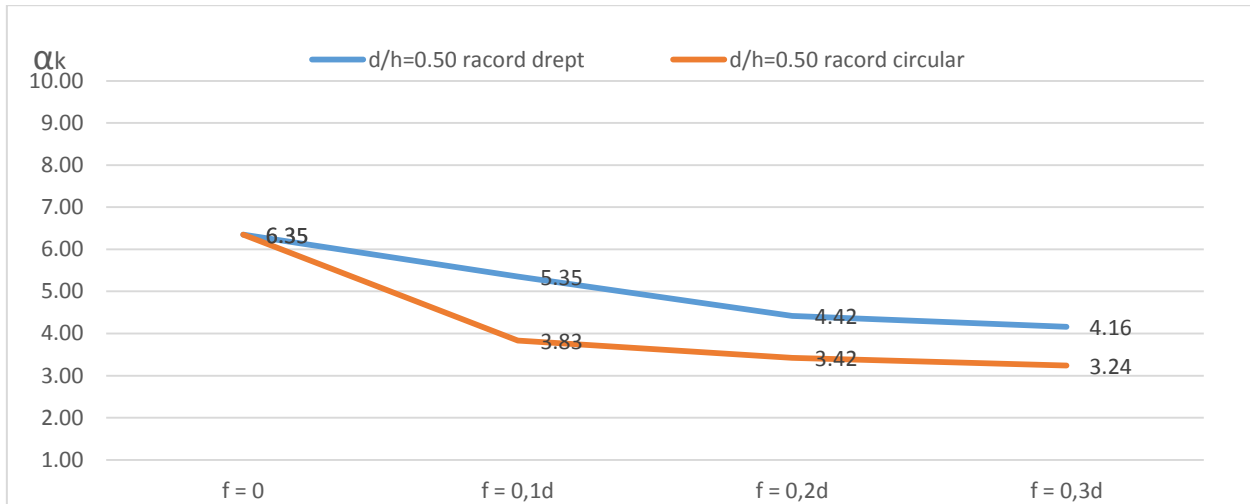


Figure 10. α_k values for $d/h = 0.50$

In Figure 10 are shown the values of α_k for central hole size $d / h = 0.50$ for both circular joints and chamfered joints. Note that the maximum values for α_k is when $f = 0$. α_k values are higher in the case of chamfered joints than in the case of circular joints with values of α_k lower with 39,69% in the case of chamfer joints for $f = 0.1d$, 29,24% for $f = 0.2d$ and 28,40% for $f = 0.3d$. Note in both cases a decrease α_k coefficient around rectangular holes with increasing size of the joint dimension.

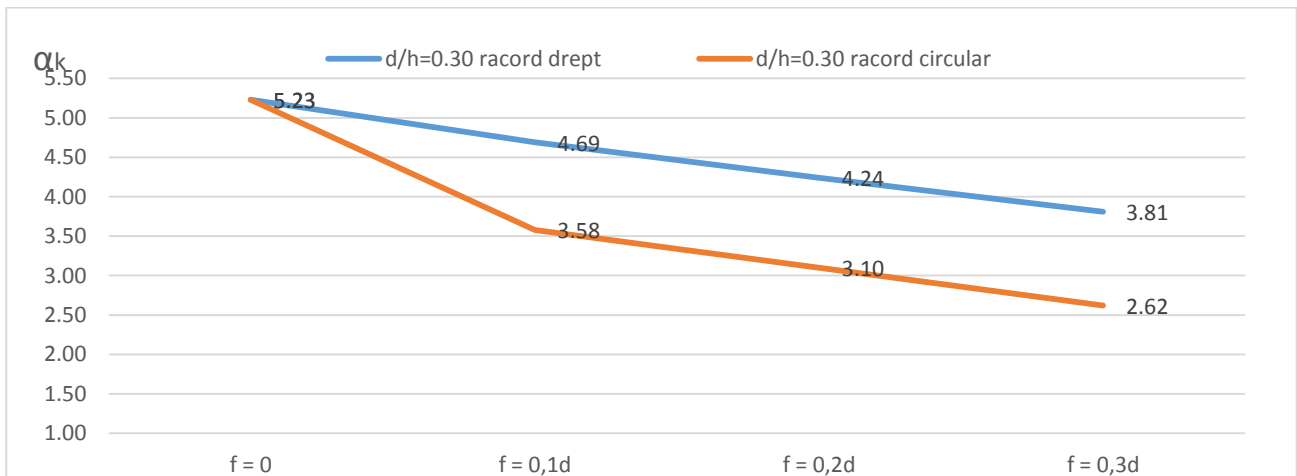


Figure 11. α_k values for $d/h = 0.30$

In Figure 11 are shown the values of α_k for central hole size $d / h = 0.30$ for both circular joints and chamfered joints. Note that the maximum values for α_k is when $f = 0$. α_k values are higher in the case of chamfered joints than in the case of circular joints with values of α_k lower with 31,01% in the case of chamfer joints for $f = 0.1d$, 42,50% for $f = 0.2d$ and 45,42% for $f = 0.3d$. Note in both cases a decrease α_k coefficient around rectangular holes with increasing size of the joint dimension.

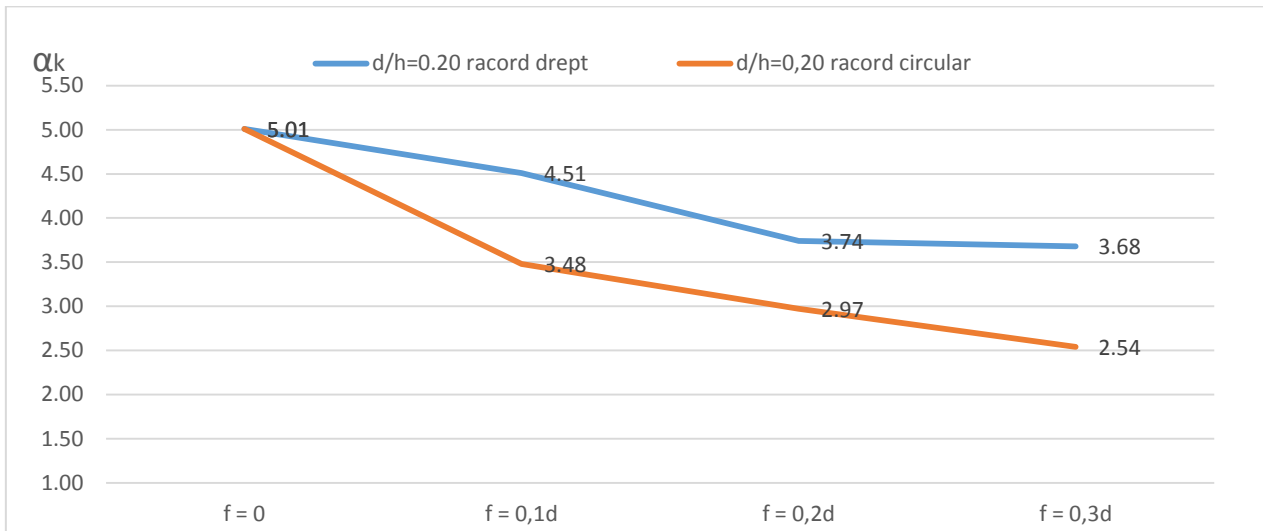


Figure 12. α_k values for $d/h = 0.20$

In Figure 12 are shown the values of α_k for central hole size $d / h = 0.20$ for both circular joints and chamfered joints. Note that the maximum values for α_k is when $f = 0$. α_k values are higher in the case of chamfered joints than in the case of circular joints with values of α_k lower with 29,60% in the case of chamfer joints for $f = 0.1d$, 25,93% for $f = 0.2d$ and 44,86% for $f = 0.3d$. Note in both cases a decrease α_k coefficient around rectangular holes with increasing size of the joint dimension.

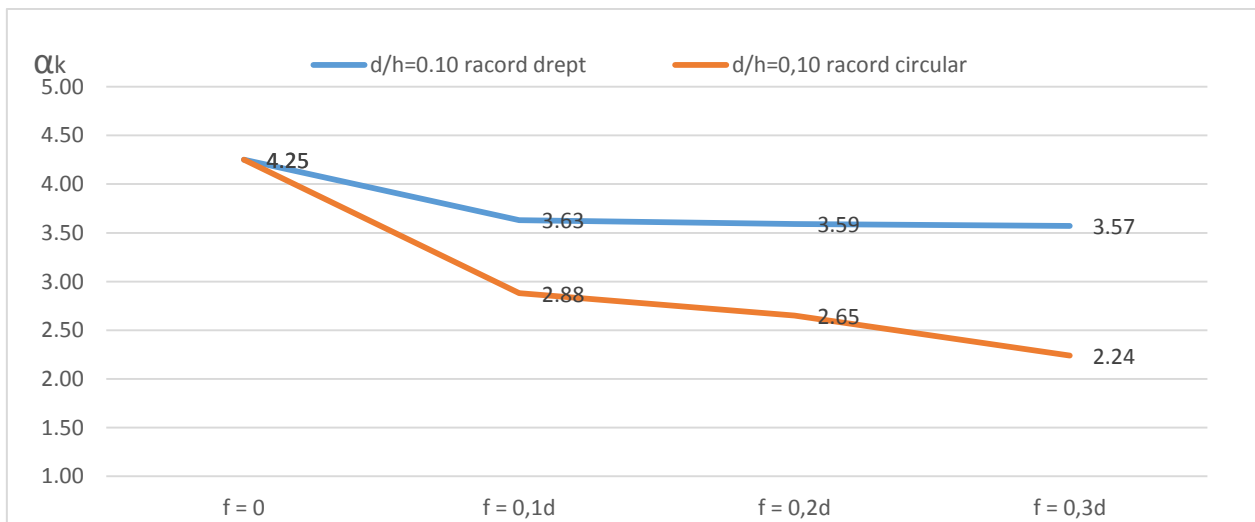


Figure 13. α_k values for $d/h = 0.10$

In Figure 13 are shown the values of α_k for central hole size $d / h = 0.10$ for both circular joints and chamfered joints. Note that the maximum values for α_k is when $f = 0$. α_k values are higher in the case of chamfered joints than in the case of circular joints with values of α_k lower with 26,04% in the case of chamfer joints for $f = 0.1d$, 35,40% for $f = 0.2d$ and 59,38% for $f = 0.3d$. Note in both cases a decrease α_k coefficient around rectangular holes with increasing size of the joint dimension.

3. Conclusion

In all five cases studied, we observe that it is more advantageous to use circular joints between the sides of rectangular holes because we obtain lower stress values around them. Sometimes there are considerable differences between values of the stresses for the two types of joints, as shown in the previous graphs. For all dimensions studied we obtained lower stress values along with increasing

the joint dimension in both cases.

From the graphs we deduce a considerable influence of chamfered joints size on coefficient α_k in all studied cases. It can also be observed that the relation between size of rectangular holes and stress values is proportional.

4. References

1. **Ille, Vasile și Bia, Cornel.** *Rezistența Materialelor vol. I.* Cluj-Napoca : Institutul Politehnic Cluj, 1969.
2. **Bia, Cornel, Ille, Vasile și Soare, M.V.** *Rezistența Materialelor și Teoria Elasticității.* București : Editura Didactică și Pedagogică, 1983.
3. **Bia, Cornel.** *Teoria Elasticității și Plasticității.* Cluj-Napoca : I.P.C.N., 1980.
4. **N. I., Bezuhov.** *Teoria Elasticității și Plasticității.* București : Editura Tehnică, 1957.
5. **Gere, J. M.** *Mechanics of Materials.* s.l. : Thomson Learning, 2004.
6. **Pilkey, Walter D.** *Peterson's Stress Concentration Factors.* New-York : John Wiley & Sons, 2nd Ed 1999. ISBN 0-471-53849-3.
7. **Soare, M.V.** *Rezistența materialelor. Curs și aplicații.* București : Institutul de Construcții București, vol.I 1978, vol.II 1978, vol.III 1982.
8. **Ille, Vasile.** *Rezistența Materialelor Partea I - Ediția a 2-a.* Cluj-Napoca : U.T. PRESS, 2011. ISBN 978-973-662-643-2.
9. **Bathe, K.J.** *Finite Element Procedures.* Englewood Cliffs, NJ : Prentice Hall, 1995.
10. **Arora, J.S.** „*Structural Design Sensitivity Analysis: Continuum and Discrete Approaches*” in *J. Herskovits (ed.) 1995 Advances in Structural Optimization pp. 47-70.* Dordrecht, The Netherlands : Kluwer Academic Publishers, 1995.
11. **Kamat, M.P.** *Structural Optimization: Status and Promise, AIAA Series in Aeronautics and Astronautics, Vol.150 pp. 851-863.* Washington, DC : American Institute for Aeronautics and Astronautics, 1993.
12. **Pilkey, W.D. și Wunderlich, W.** *Mechanics of Structures, Variational and Computational Methods.* Boca Raton FL. : CRC Press, 1993.